Supramolecular Dye Inclusion Single Crystals Created from 2,3,6-Trimethyl-β-cyclodextrin and Porphyrins
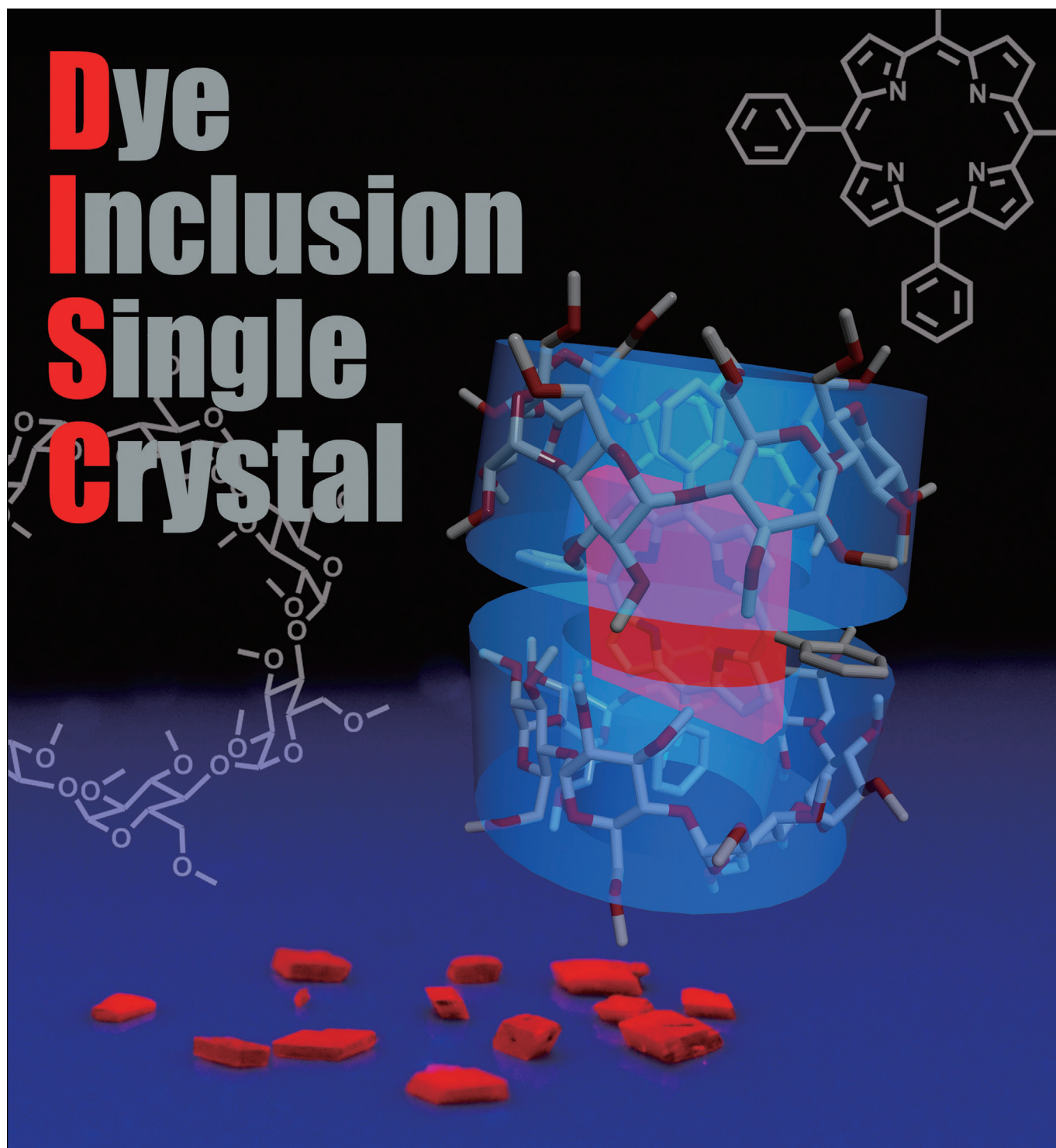
Youichi Tsuchiya,[a, b] **Tomohiro Shiraki,**[a, b] **Takashi Matsumoto,**[c] **Kouta Sugikawa,**[b, d] **Kazuki Sada,**[d] **Akihito Yamano,**[c] **and Seiji Shinkai**[a, e, f]

Abstract: In Nature, chromophoric groups play various roles, such as oxygen carriers, electron donors, light sensitizers, which are achieved in many cases by control of their aggregation modes in proteins. Host–guest chemistry between cyclodextrins and porphyrins has attracted great interest from supramolecular chemists because of their unique structures and functions that mimic those of proteins with chromophoric prosthetic groups. To mimic Nature's contrivances, the host–guest systems between cyclodextrins and porphyrins have frequently been studied.

It is really surprising, however, that to date no detailed structural information of these complexes has been obtained from single-crystal analysis. In 2011, we reported the first successful isolation of a dye inclusion single crystal (DISC) between 2,3,6-trimethyl-β-cyclodextrin (TMβCD) and 5,10,15,20-tetrapyridyl-porphyrin (TPyP), and analyzed its

X-ray crystal structure. The crystal structure revealed not only the real complex mode but also the attractive orientation of TPyP in the DISC. Herein, we present new strategies to prepare DISCs of TMβCD for several porphyrins and provide crystal structures, details of the complex modes, and optical properties. We believe that the present study has various important implications not only for the basic crystal analysis of inclusion complexes but also for potential applications that use these single crystals.

Introduction

In the research into photon-to-electron conversion mediated by dye molecules, we always meet one inevitable dilemma: in general, high light-absorption efficiency is achieved with densely packed dye assemblies, whereas the energy of the photoexcited state is consumed by concentration quenching.[1] To avoid undesirable quenching phenomena, we have

[a] Dr. Y. Tsuchiya, Dr. T. Shiraki, Prof. S. Shinkai
Nanotechnology Laboratory
Institute of Systems, Information Technologies and Nanotechnologies (ISIT)
203-1, Moto-oka, Nishi-ku, Fukuoka 819-0385 (Japan)
Fax: (+81) 92-805-3814
E-mail: tsuchiya@isit.or.jp
        shinkai_center@mail.cstm.kyushu-u.ac.jp

[b] Dr. Y. Tsuchiya, Dr. T. Shiraki, K. Sugikawa
Department of Chemistry and Biochemistry
Graduate School of Engineering
Kyushu University
744, Moto-oka, Nishi-ku, Fukuoka 819-0395 (Japan)

[c] Dr. T. Matsumoto, Dr. A. Yamano
X-Ray Research Laboratory
Rigaku Corporation
3-9-12, Matsubara, Akishima, Tokyo 196-8666 (Japan)

[d] K. Sugikawa, Prof. K. Sada
Division of Chemistry
School of Science
Hokkaido University
North 10, West 8, Kita-ku, Sapporo, Hokkaido 060-0810 (Japan)

[e] Prof. S. Shinkai
Department of Nanoscience
Faculty of Engineering
Sojo University
4-22-1, Ikeda, Kumamoto 860-0082 (Japan)

[f] Prof. S. Shinkai
Faculty of Institute for Advanced Study
Kyushu University
744, Moto-oka, Nishi-ku, Fukuoka 819-0395 (Japan)

Supporting information for this article is available on the WWW under http://dx.doi.org/10.1002/chem.201102075.

to moderately dilute the density of dye molecules. The most expeditious idea would be to dilute dye molecules by mixing them with inert molecules. However, this simple idea frequently suffers from phase separation to form self-sorting dye assemblies. A more practical idea to solve this dilemma has been offered by a synthetic approach to introduce bulky substituents into the dye molecule through covalent bonds;[2] owing to their bulkiness, the distance between dye molecules is increased, but the fine tuning of this increase in distance by substituents seems to be very difficult. As a more sophisticated solution, one can employ a supramolecular approach, that is, encapsulation of a dye molecule by a host molecule. In this method, the dye molecules in the complex are insulated from each other even in densely packed complex assemblies. As examples for such encapsulation, Fujita et al. synthesized networked molecular cages as crystalline sponges for fullerenes and other guests.[3] Similarly, García-Garibay et al. designed crystals called molecular gyroscopes, in which functional guests are encapsulated by covalent bonds.[4] We also included fullerenes in a dimeric homooxacalix[3]arene capsule and succeeded arranging the complexes on an indium tin oxide surface to fabricate a solar cell model.[5] One may observe that Nature also adopts this strategy in photosynthetic systems: the chlorophyll–chlorophyll interaction is suppressed by encapsulation in protein matrices and 35 chlorophylls are arranged in a designed aggregation mode in Photosystem II (PSII), a membrane protein complex composed of 19 protein subunits.[6] PSII can achieve, therefore, a highly efficient energy conversion from light to chemical energy. Many researchers have been inspired by this Nature-designed supramolecular system and have so far constructed various artificial photosynthetic or light-to-electric current conversion systems, in which the abilities inherent to porphyrins have played central roles.[7] In the opto-electrochemical research field, it is well established that the insulation of each porphyrin and the control of the aggregation mode are decisive factors that improve the light-harvesting efficiency.[8] Here, it occurred

to us that the crystal phase of cyclodextrin (CD) inclusion complexes might be a potential and expeditious alternative to realize a variety of regularly oriented porphyrin assemblies, that is, our first idea was to moderately increase the distance between porphyrins through formation of inclusion complexes with CDs.

The host–guest complexes of CDs have been studied extensively over a long period.[9] In particular, the interaction between β-cyclodextrins (β-CDs) and porphyrins has been attractive research targets from the viewpoint of various biomimetic models for hemoproteins, PSII, etc.[10] We reported an artificial photosynthetic system using porphyrins in which the electron transfer efficiency is much improved by complexation with β-CD.[11] These research ideas stem from the fact that β-CD and its derivatives have a strong binding ability for water-soluble porphyrins.[12–15] In particular, 2,3,6-trimethyl-β-cyclodextrin (TMβCD) has a higher inclusion affinity for the *meso*-aryl group of tetraarylporphyrins ($K \approx 10^6 \, M^{-1}$) than other CDs.[13] This difference is attributed to the ring flexibility inherent to TMβCD, which originates from the loss of the intramolecular hydrogen bonds between OH groups. As a result, TMβCD can undergo induced-fit-type complexation with various guest molecules. Despite their known properties in solution, to the best of our knowledge there was no preceding report of a single-crystal analysis of the inclusion complex between TMβCD and porphyrins until our communication appeared in 2011.[16] Since 1990, the complexes formed between β-CDs and porphyrins have been proposed to be a 2:1 bicapped inclusion structure in aqueous solution.[14] In these reports, however, the structures of the complexes have been discussed only on the basis of the spectral properties in solution and theoretical calculations. It is really surprising that so far, nobody knows the real complex structure determined from single-crystal analysis, although the complexation modes have frequently been discussed in the references. In our recent communication,[16] we reported the single-crystal structure for the inclu-

sion complex of 5,10,15,20-tetrapyridylporphyrin (TPyP) bicapped with TMβCD. It is the first successful example of a dye inclusion single crystal (DISC) between CDs and porphyrins. The key points for the successful isolation of a high-quality single crystal were: 1) a pH-dependent solubility change for the porphyrin; 2) the flexibility of TMβCD, which enabled an induced-fit-type guest inclusion ability; and 3) a higher crystal-growth temperature, which is advantageous for the hydrophobic force that acts as the driving force of inclusion. Herein, we report DISCs for the TMβCD complexes with five different porphyrins, including one metalloporphyrin (Figure 1), and their preparation, structural characteristics, and optical properties. The results indicate that these complexes possess significant potential for application in new opto-electronic materials.

Results and Discussion

Preparation of porphyrin inclusion crystals: TPyP is scarcely soluble in water. In this case, even though β-CD solubilizes porphyrins into water, the crystallization treatment results in the porphyrin crystal dissociating from the complex. However, TPyP becomes water-soluble under acidic conditions owing to protonation of the *meso*-pyridyl groups. It is known, however, that the cationic *meso*-pyridiniumporphyrin shows a weak interaction with β-CD.[15] This is attributed primarily to the enhanced hydrophilicity of the *meso*-pyridinium groups and secondly to the slightly positively polarized interior cavity of the cyclodextrin. As a result, protonated TPyP shows only a low affinity for CDs. One may expect, therefore, that the binding constants would gradually increase with neutralization of the *meso*-pyridinium groups and that at some stage TPyP would become water-insoluble. However, one can expect that TPyP would be still homogeneously dispersed in the presence of excess TMβCD. Figure 2 shows the UV/Vis and circular dichroic spectra of TPyP. In acidic solution, no circular dichroic signal was observed, whereas induced circular dichroic signals clearly appear in the pH-neutral solution in the presence of excess TMβCD. It is clear, therefore, that TPyP is solubilized by the strong binding ability of TMβCD toward the neutral *meso*-pyridyl groups. In fact, an aqueous solution of TPyP with TMβCD did not give any precipitate over one year.

A TPyP·TMβCD DISC was obtained from an aqueous solution of TPyP with excess TMβCD at 60 °C (Figure S1 a in the Supporting Information). It may be a little curious that crystallization of the TMβCD·TPyP complex was performed at such high temperature. In aqueous solution, CDs and their derivatives are strongly solvated with water molecules through hydrogen-bonding interactions. Under heating, it is expected that the hydrogen bonds are cleaved and the hydrophobic nature becomes the stronger effect.[9,17] In particular, TMβCD behaves as a more hydrophobic host molecule than β-CD, and TMβCD complexes in water are more stabilized at higher temperatures, which leads to advantageous conditions for crystal growth. However, when 2,6-dimethyl-
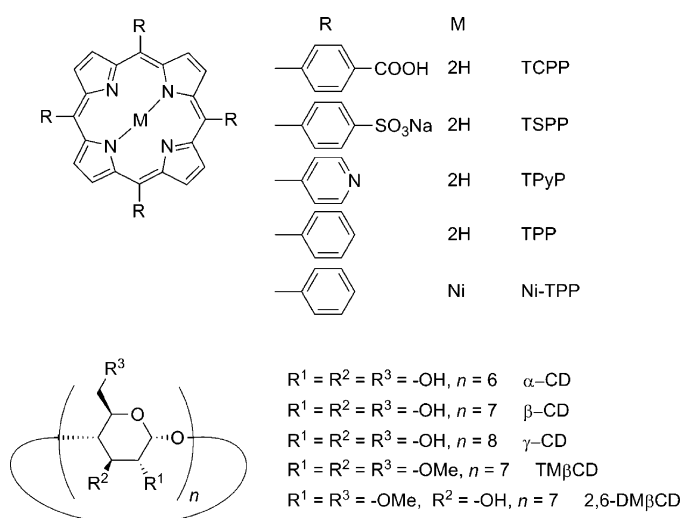

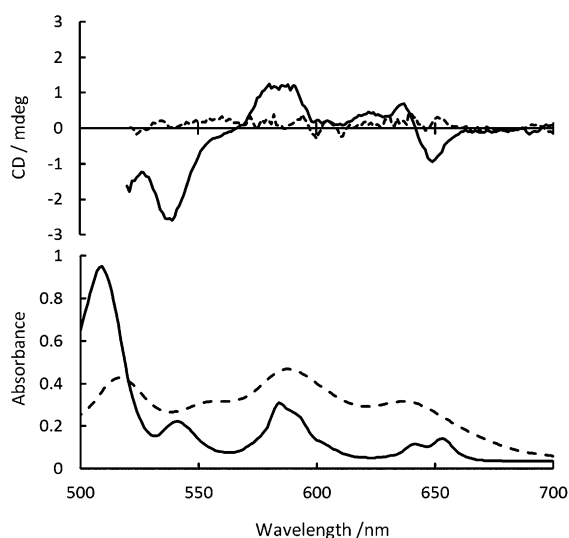Figure 1. Structures of porphyrins and cyclodextrins.

Figure 2. Circular dichroism (top; $I = 0.5$ mm) and visible (bottom; $I = 0.1$ mm) spectra of aqueous TPyP and TMβCD before (-----) and after (——) neutralization. The concentrations of TPyP and TMβCD are same as in the crystallization solution.

β-cyclodextrin (2,6-DMβCD) was used instead of TMβCD, colorless crystals of 2,6-DMβCD and micro-crystals of TPyP were obtained separately. Kano et al. reported that TMβCD has the highest inclusion affinity for the hydrophobic *meso*-aryl groups of tetraarylporphyrins ($K \approx 10^6 \, \text{M}^{-1}$) of available CDs and their methylated derivatives. In aqueous solution, the binding constants between 2,6-DMβCD and porphyrins are relatively large ($K \approx 10^4 \, \text{M}^{-1}$), but they are smaller by two orders of magnitude than those of TMβCD.[14] This difference can be explained by the rigidity of the cyclodextrin rings. Results of NMR spectroscopy studies rationally explain the high inclusion ability of TMβCD, that is, induced-fit-type complex formation is operative between TMβCD and tetraarylporphyrins. However, β-CD and 2,6-DMβCD are classified as rigid hosts, the complex structures of which are more or less affected by the intramolecular hydrogen bonding between the secondary hydroxyl groups. For these reasons, it seems difficult to isolate pure single crystals of the inclusion complexes of β-CD and 2,6-DMβCD from aqueous solution. We now consider that the structural flexibility of host molecules is an important factor in the growth of single crystals of inclusion complexes.

We have succeeded in isolating DISCs from complexes with other several porphyrins. 5,10,15,20-Tetrakis(4-carboxy-phenyl)porphyrin (TCPP) is another water-soluble porphyrin that shows a pH-dependent solubility change similar to TPyP, that is, TCPP can be solubilized into water by alkaline dissociation of the carboxylic acid groups. In the solution state, there are several preceding studies on the inclusion complex between TMβCD and TCPP.[10, 12] The association constants are $K_1 = 1.7 \times 10^4 \, \text{M}^{-1}$ (for a 1:1 complex) and $K_2 = 2.0 \times 10^5 \, \text{M}^{-1}$ (for a 1:2 bicapped complex) in aqueous buffer solution at pH 7.[12f] We thought that gradual acid neutralization of the dissociated carboxylate groups would further en-

hance the association constants. A DISC of TMβCD·TCPP complex was obtained from an aqueous solution of TCPP containing an excess amount of TMβCD at 50 °C (Figure S1 b in the Supporting Information). The TMβCD·TCPP DISC appeared as hexagonal platelet crystals that grew into hexagonal rod-like crystals with further incubation. The rod-like crystals obtained by isolation from the crystalline solution were easily decomposed along the crystal-growth direction to give platelet crystals (Figure S2 in the Supporting Information). The crystal structure of the hexagonal platelet could not be analyzed clearly because of its low resolution. Herein, this kind of transitional crystal growth was observed only for the TCPP complex, but not for other DISCs. For the highly water-soluble 5,10,15,20-tetrakis(4-sulfonatophenyl)porphyrin (TSPP), it was difficult to isolate the DISC by using the same procedure. Thus, we prepared a high salt concentration solution from which a powder of the inclusion complex could be isolated above 80 °C. However, the crystal quality was not sufficient for X-ray analysis.

Because 5,10,15,20-tetraphenylporphyrin (TPP) with hydrophobic *meso*-phenyl groups is sparingly soluble in water, it seems difficult to form an inclusion complex according to the procedure described above. However, it occurred to us that the preparation method for formation of a host–guest complex between γ-cyclodextrin (γ-CD) and hydrophobic fullerene C60 might be applicable to our system. Komatsu et al. reported that supramolecular complexation of fullerenes with γ-CD was possible by mechanical shaking.[18] We thus applied this mechanochemical method to the preparation of an inclusion complex with hydrophobic porphyrins. Microcrystals of TPP and excess TMβCD were finely ground in an agate mortar. After dispersing the ground mixture into water with stirring, the cloudy solution was filtered to obtain a clear solution that contained the inclusion complex. Then, the TMβCD·TPP DISC was obtained by keeping the solution at 50 °C (Figure S1 c in the Supporting Information). The Ni[II]-coordinated TPP (Ni-TPP) DISC was also obtained by using this procedure (Figure S1 d in the Supporting Information). The results imply that this method is widely applicable to complex formation between CDs and hydrophobic guests.

Structural considerations of inclusion crystals: The crystal structures of the TMβCD·porphyrin complexes are shown in Figure 3. Regardless of the difference in the *meso*-aryl groups, all complex structures consist of one porphyrin capped with two TMβCD molecules. In addition, two *meso*-aryl groups of the guest porphyrins penetrate into the TMβCD cavity from the O2, O3 side to the O6 side. This feature of the bicapped host–guest complex structures is consistent with that proposed, so far, for the solution complexes on the basis of the spectral studies.[12–15] Table 1 shows the details of the crystal parameters. It can be seen that the crystal system of the TMβCD·TCPP complex is different to the other three porphyrins. DISCs of TPyP, TPP, and Ni-TPP complexes commonly adopt triclinic crystalline systems that are remarkably similar to one another, whereas
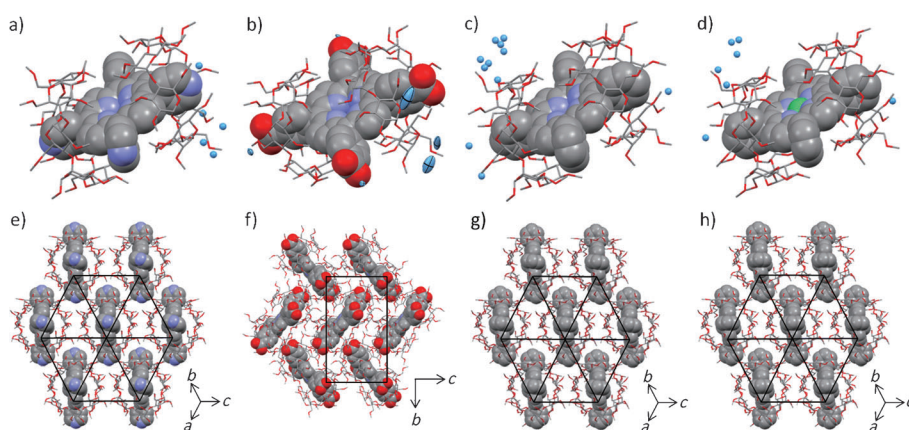
Figure 3. Crystal structures of the unit cells of a) TMβCD·TPyP, b) TMβCD·TCPP, c) TMβCD·TPP, and d) TMβCD·Ni-TPP DISCs. Hydrogen atoms are omitted for clarity. Water molecules of crystallization are illustrated as light blue ellipsoids (occ. = 1.0) or balls (occ. < 0.5). Molecular packing of e) TMβCD·TPyP, f) TMβCD·TCPP, g) TMβCD·TPP, and h) TMβCD·Ni-TPP DISCs viewed along the (111) or (100) plane. Hydrogen atoms and water molecules of crystallization are omitted for clarity.

Table 1. Details of the crystal structures of DISCs between TMβCD and various porphyrins.

	TMβCD·TPyP	TMβCD·TCPP	TMβCD·TPP	TMβCD·Ni-TPP
M_r	3477.77	3745.90	3473.86	3530.55
crystal color, habit	red, platelet	red, platelet	red, platelet	red, platelet
crystal system	triclinic	monoclinic	triclinic	triclinic
space group	$P1$	$P2_1$	$P1$	$P1$
Z	1	2	1	1
total water of crystallization[a]	1	6	3	1.4
found water molecules[b]	5	6	11	7
a [Å]	16.864(4)	16.983(2)	16.8100	16.782(3)
b [Å]	17.532(4)	28.298(3)	17.9010	17.880(3)
c [Å]	17.17.712(4)	20.715(2)	17.7910	17.794(3)
α [°]	98.9688(10)		98.0900	98.078(2)
β [°]	103.336(3)	104.018(2)	102.3700	102.593(2)
γ [°]	112.9167(2)		114.4900	114.384(2)
V [Å³]	4514(2)	9659(2)	4597.4571	4583.5(12)
ρ_{calcd} [g cm⁻³]	1.279	1.288	1.255	1.279
twist angle of porphyrin[c] [°]	7.3	7.3	7.3	9.1
decomposition point[d] [°C]	198–202	183–190	197–205	184–186

[a] Total number of water molecules of crystallization determined from their occupation probabilities in the unit cell. [b] Number of found water molecules determined from their occupation probabilities in the unit cell. [c] The twist angles of the porphyrins were measured from the top view of the crystal structure of their DISCs. [d] Decomposition points were determined by visual observation method by using melting-point apparatus.

TMβCD·TCPP DISCs have a monoclinic crystalline system. In addition, the volume of the TMβCD·TCPP crystal lattice was estimated to be two times larger than those of other three porphyrin complexes. Careful examination of the crystal structures (Figure 3e–h) reveals the origin of this difference: in TPyP, TPP, and Ni-TPP complexes, the porphyrins are arranged unidirectionally and maintain a periodical distance, whereas the TMβCD·TCPP complex adopts an alternate orientation. Thus, the crystal structure of the

TMβCD·TCPP complex has a twofold rotational symmetry. We considered that this unique alternate orientation stems from the hydrogen-bonding framework that extends between the carboxyl groups of TCPP, the water molecules, and the methoxy group oxygen atoms of TMβCD. In fact, we note the presence of six water molecules in the TMβCD·TCPP complex structure (Figure 3). Their respective occupation probability is 1.0, whereas the respective occupation probabilities of all water molecules in other three complexes are much lower (<0.5) than this value. Figure 4 shows the results of differential scanning calorimetry for the crystals of TMβCD·TCPP and TMβCD·TPyP. For TMβCD·TPyP, an endothermic peak is observed at 195°C, which is assigned to a decomposition point of this complex. In contrast, TMβCD·TCPP shows an additional peak at 45°C, in addition to a decomposition point at 182°C. In the thermogravimetric analysis measurement, a crystal weight decrease of 4% was observed at around 45°C. With heating above 75°C, the crystals of TMβCD·TCPP crumbled to powder and the color changed from brown to dark red. The room-temperature IR spectrum of TMβCD·TCPP shows a broad peak at 3430 cm⁻¹ that was assigned to O−H stretching. After heating above 75°C, however, no peak appears in this region (Figure S3 in the Supporting Information). These results consistently indicate that water molecules play an important role in the formation of a well-arranged TMβCD·TCPP crystal structure.

The decomposition point of TMβCD·TCPP appears in a lower temperature region with a peak sharper than that of TMβCD·TPyP. We can rationalize this difference as follows: as the crystal structure of TMβCD·TCPP is partly disordered by dehydration and changes to the powder, TMβCD acquires more freedom even in the solid phase. In contrast, TMβCD·TPyP is very well stabilized not only by the complex formation energy but also by the crystal packing. Thus, the decomposition point of TMβCD·TCPP appears at a lower temperature than that of TMβCD·TPyP. However, the decomposition point of TMβCD·Ni-TPP was lower than that of TMβCD·TPP. This shift is ascribed to the larger twisted angle of Ni-TPP in the solid state compared with TPP and TPyP (see below).
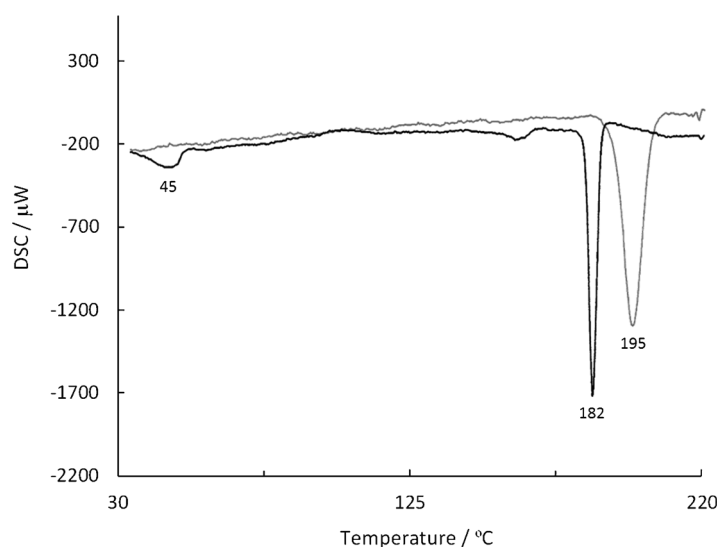
Figure 4. a) Differential scanning calorimetry of TMβCD·TPyP (——) and TMβCD·TCPP (——) DISCs.

Structural considerations of cyclodextrin–porphyrin inclusion complexes: So far, the structure of cyclodextrin–porphyrin complexes has been proposed only for the solution state on the basis of the spectroscopic studies.[12–15] For example, Kano et al. reported that a stronger interaction operates between porphyrins and β-CD, which consists of seven glucose units, than between porphyrins and α-CD or γ-CD, which consist of six or eight glucose units, respectively.[13] In particular, *O*-methylation of secondary hydroxyl groups in β-CD further intensifies its guest-binding ability. An explanation of this change on the basis of ^{13}C NMR spectral data is that formation of the inclusion complex is facilitated by a induced-fit-type host–guest interaction because the loss of intramolecular hydrogen bonding through *O*-methylation makes the CD ring considerably more flexible and the NMR signals are significantly shifted upon guest inclusion. We presume that this induced-fit is associated with distortion of the β-CD ring with respect to the π plane of the included porphyrin. In our structural analysis, it is not so clear from

the top view (Figure 5) whether or not TMβCD is significantly distorted along the porphyrin. More obvious is the finding that the π system of the porphyrin ring is twisted to the left by 7.3°, which is a general trend for all free-base porphyrin complexes. Interestingly, the twisted angle of Ni-TPP is increased up to 9.1°. However, the significant difference in the crystal packing between TMβCD·TPP and TMβCD·Ni-TPP was not observed, except for the twist angle of porphyrins (Table 1). It is known that certain metalloporphyrin planes, such as Ni-TPP, are more distorted than free-base porphyrins.[19] This trend can be further emphasized in the DISC.

Moreover, we noticed a significant structural difference between TMβCD·TCPP and the other complexes. The position of glucose units in TMβCD with respect to the included porphyrin could be assigned by using the position of glucoside oxygen atoms linking the glucose units together. In TMβCD·TPyP and TMβCD·TPP, the glucose units on upper and lower TMβCDs occupy almost regularly aligned positions between the two TMβCDs in the top view. Conversely, their positions in TMβCD·TCPP are not aligned but rather appear to alternate. However, all free-base porphyrins are equally twisted to the left by 7.3° in their DISCs. So far, it
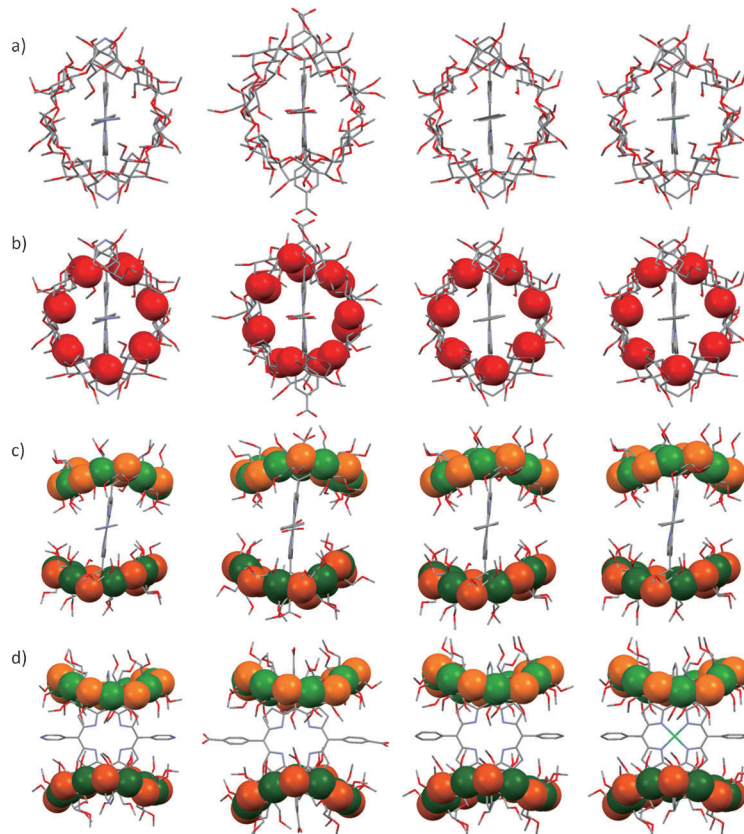

Figure 5. Crystal structures of TMβCD·TPyP, TMβCD·TCPP, TMβCD·TPP, and TMβCD·Ni-TPP DISCs (left–right); a) top view, b) top view with the oxygen atoms of the glycoside bond shown as red balls, c) side view with C1 and C4 atoms shown as orange and green balls, respectively, d) front view with C1 and C4 atoms shown as orange and green balls, respectively. Hydrogen atoms and water molecules of crystallization are omitted for clarity.

was noted that the twisted π system of porphyrins is induced by steric crowding that arises from the positional relationship between the porphyrin and the glucoses of TMβCD.[16] However, this is not always correct. We find an alternate, very important common structural characteristic of the inclusion complexes in the side view and front view. These structures are illustrated in Figure 5, and emphasize the C1 and C4 atoms connected to the glucoside oxygen atoms. One can clearly see that strains in the glucose ring belt occur. Probably, this type of strain is more advantageous than cyclodextrin ring strain along the porphyrin to enhance the hydrophobic contact with porphyrins. This bent structure is commonly seen for all inclusion complexes. Thus, we now consider that this is the essential character of induced-fit-type interactions. In addition, Kano et al. reported that the bent structure of permethylated CDs that have no OH groups plays an important role in chiral recognition.[20] It is reasonable to consider, therefore, that the considerably bent structure of each glucose ring belt should induce chiral twisting of the porphyrin π system, which eventually leads to chiral recognition.

Optical properties of porphyrin inclusion crystals: We found that the DISC of TMβCD·TPyP shows unique optical anisotropy (Figure 6). The oblique extinction was observed under
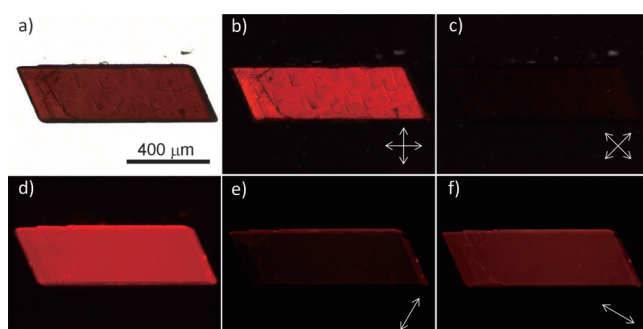

Figure 6. Microscope images of the TMβCD·TPyP DISC; a) bright-field image, b) crossed Nicols polarized image (0–90°), c) crossed Nicols polarized image (45–135°), d) fluorescent image, e) fluorescent image with polarizer (60°), and f) fluorescent image with polarizer (150°).

crossed Nicol prisms. The extinction angle used for this experiment was 45°. In one Nicol observation, the extinction of polarized light was observed at 135° with respect to the major axis of the crystal. This angle lies approximately evenly between the major and minor axes. More interestingly, when the fluorescence was observed through the polarizer, the fluorescence intensity was minimized at around 60° and maximized at around 150° for the major axis of the crystal. These findings can be explained rationally by the neat arrangement of TPyP molecules in the crystal. Figure 7 shows the arrangement of porphyrin molecules viewed along the (001) plane (see Figure S4 in the Supporting Information for the relationship between the crystalline lattice and the reciprocal lattice). It is easily observed that the angles of the *meso*-axis of TPyP with respect to the *a* axis
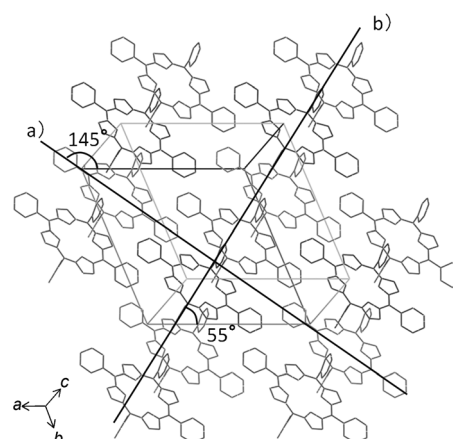

Figure 7. Arrangement of TPyP molecules in the TMβCD·TPyP DISC viewed along the (001) plane. a) *meso*-Axis of TPyP that provides the maximum polarized fluorescence. b) *meso*-Axis of TPyP that provides the minimum polarized fluorescence.

are similar to the angles of maximum and minimum intensity of the liner polarized fluorescence with respect to the major axis of the crystal. If one *meso*-axis has an angle of 55° with respect to the major axis of the crystal, TPyP is tilted around 56° towards the (001) plane. In contrast, if the other *meso*-axis has an angle of 145° with respect to the major axis of the crystal, TPyP is arranged almost parallel (<2°). In addition, the DISC of TPP, which has a crystal structure similar to the DISC of TPyP, showed the same optical properties (Figure S5 in the Supporting Information). This characteristic alignment of porphyrins should be mainly associated with linearly polarized luminescence properties. The DISC of Ni-TPP, which is known to be nonfluorescent, showed the same optical anisotropy. On the other hand, significant optical anisotropy was not observed for TMβCD·TCPP. This difference is likely to be associated with the difference in the arrangement of porphyrins in the DISC, that is, whether they are unidirectional or not.
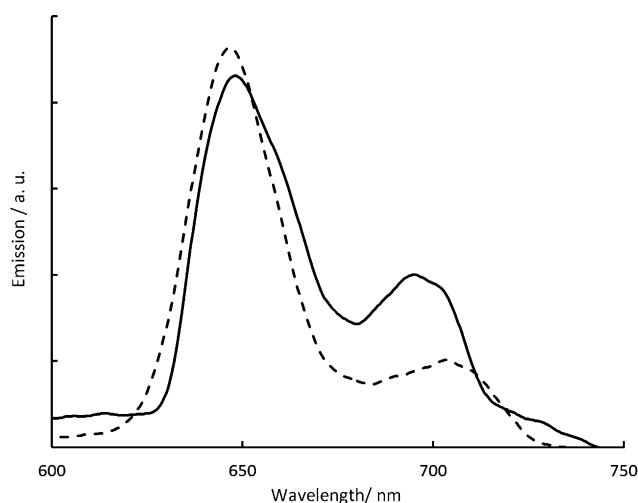

Figure 8. Fluorescence spectra of TMβCD·TPyP in aqueous solution (----; [2TMβCD·TPyP] = 6.6 μM) and DISC (——); λ_{ex} = 510 nm.

Figure 8 shows the fluorescence spectra of TMβCD·TPyP in the aqueous solution phase and in the DISC phase. The fluorescence quantum yields were estimated to be 5.2 and 3.5%, respectively. In the solution phase, the fluorescence intensity ratio of the higher peak ($\lambda_{em} = 704$ nm) versus lower peak ($\lambda_{em} = 647$ nm) was 0.22. Conversely, the peak ratio in the DISC phase was 0.47 ($\lambda_{em} = 695$ and 650 nm). One may consider that the change in the fluorescence peak ratio and the shift are induced by the porphyrin structure being fixed in the CD cavity. To obtain further insight into the association mode, we measured the fluorescence lifetime of TMβCD·TPyP in the aqueous solution phase and the DISC phase (Figure 9). Table 2 shows the results obtained
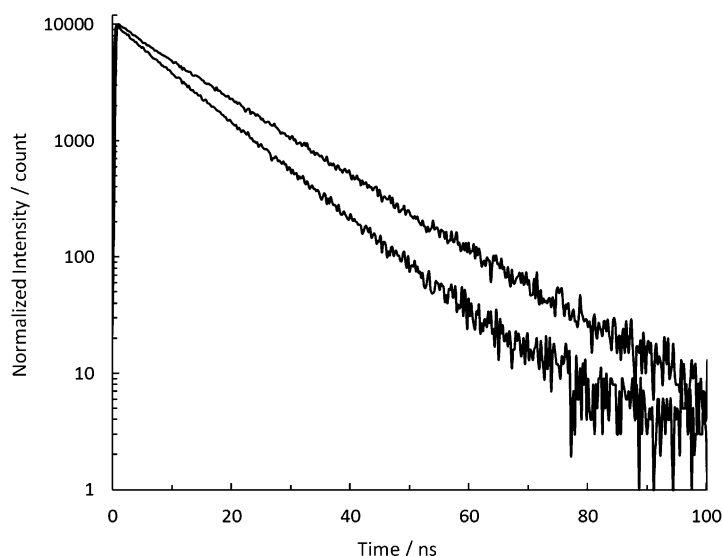

Figure 9. Fluorescence decay curves of TMβCD·TPyP complex in aqueous solution ([2 TMβCD·TPyP] = 6.6 μM) and DISC at $\lambda = 705$ nm.

Table 2. Fluorescence lifetimes of TMβCD·TPyP.

State	λ [nm]	t_1 [ns]	t_2 [ns]	Φ_T [%]
aqueous solution[a]	650	11.8	2.7	5.2[b]
	705	13.2	1.3	
DISC	650	9.9	–	3.5[b]
	705	10.3	–	
Ref. [20]	650	12.5	0.5	–
	705	12.5	0.03	

[a] 1000 times more dilute than the crystallization solution ([2 TMβCD·TPyP] = 6.6 μM). [b] Total light quantum yield was measured in the range of $\lambda = 594$–768 nm with monochromatic light excitation ($\lambda = 510$ nm, range: $\lambda = 500$–520 nm).

by monitoring at $\lambda = 650$ and 705 nm. Clearly, the fluorescence lifetime in the DISC phase is shorter than that of the solution phase. Takagi et al. previously reported that porphyrins can be regularly arranged on a clay sheet to act as an inorganic host.[22] In their study, the distance between porphyrins was estimated to be about 2.4 nm. Importantly, they found that the energy transfer between porphyrins can take place very efficiently. In the TMβCD·TPyP DISC, the

distance from one porphyrin to neighboring porphyrins is estimated to be between 1.7 and 2.9 nm. However, all porphyrins can be connected, in a stepwise manner, by less than 1.8 nm.[16] One may propose from these reasons that the shorter fluorescence lifetime of the DISC phase is rationalized in terms of the energy transfer between neighboring porphyrins.

Conclusion

Herein, we demonstrate a new strategy to isolate DISCs formed between TMβCD and several porphyrins with different *meso*-aryl groups or a coordinated metal. We obtained high-quality DISCs regardless of the water solubility of the porphyrin used. The key points in this preparation method are the flexibility of TMβCD, which enables induced-fit-type guest inclusion, and a high-temperature crystallization, which is advantageous for the hydrophobic force to dominate. We have examined the structural characteristics of these induced-fit-type complexation modes in the DISC phase for the first time. Particularly important is our finding that complexation induces bending of the glucose ring belt structure in the cyclodextrin but not strain of the cyclodextrin ring structure itself along the π plane of the included porphyrin, as predicted from solution studies. The bent structure of the CDs was not significantly affected by different *meso*-aryl groups on the porphyrin. In TCPP, the hydrogen bonds between TMβCD, water molecules, and carboxyl groups play an important role in forming the crystal structure. As a result, only TMβCD·TCPP was oriented in a nested structure in the DISC, whereas other porphyrin complexes were oriented unidirectionally. Thus, the molecular orientation in the crystals should be controlled by the nature of the *meso*-aryl groups. In addition, we found that the bent structure in the complexes results in a chirally twisted π plane in the guest porphyrins. This twisting angle could be also controlled by introduction of metals into the porphyrins because the twisting angle of the Ni-TPP complex is significantly larger (by 1.8°) than those of other free-base porphyrins. Furthermore, we have demonstrated the potential application of DISCs in electrochemical and optoelectronic materials. We thus believe that the present study has various important implications not only for basic crystal analysis of inclusion complexes but also for applied research that uses the concept of supramolecular chemistry.

Experimental Section

Preparation of TMβCD·TCPP DISCs: TCPP (79 mg, 0.1 mmol) and TMβCD (572 mg, 0.4 mmol) were dissolved in aqueous NaOH (5 mL; 1 mol dm⁻³). After neutralizing with aqueous HCl (5 mL, 1 mol dm⁻³),

the volume of the solution was adjusted to 15 mL by addition of water. The DISC was obtained by incubation at 50°C for 3 d.

Preparation of DISCs of TMβCD and hydrophobic porphyrins: TPP (31 mg, 0.05 mmol) or Ni-TPP (33.6 mg, 0.05 mmol) was finely ground in an agate mortar with excess TMβCD (429 mg, 0.3 mmol). After dispersing the ground mixture into water with stirring, the cloudy solution was filtered to obtain a clear solution that contained the inclusion complex. The DISCs corresponding each porphyrin inclusion complex were obtained by incubation at 50°C for 3 d.

Instruments: UV/Vis spectra were measured by using a JASCO V-670 spectrophotometer. Circular dichrovism spectra were measured by using a JASCO J-720WI spectropolarimeter. DSC thermograms were recorded by using a Seiko Instruments SSC 5200 (type DSC 220C) thermal analysis system. Fluorescence spectra were measured by using a Perkin–Elmer LS 55 luminescence spectrometer. Quantum yields were recorded by using an integrating sphere and a Hamamatsu Photonics C10027 photonic multi-channel analyzer. The fluorescence decay measurements were carried out by using the time-correlated single-photon counting technique by using a Horiba–Jobin–Yvon FluoroCube 3000U lifetime spectrofluorometer system equipped with a Horiba Scientific Nano-LED-375L pulsed diode light source.

X-ray crystallography: X-ray analytical data were collected by using a Saturn 724+ diffractometer with multilayer mirror monochromated $Mo_{K\alpha}$ radiation (Rigaku). The reflection data were collected and processed by using CrystalClear (Rigaku). The structures were solved by direct methods and expanded by using Fourier techniques. Some nonhydrogen atoms were refined anisotropically, whereas the rest of the atoms were refined isotropically. Hydrogen atoms were refined by using a riding model. The final cycle of full-matrix least-squares refinement on F^2 based on unique reflections was employed, in which the unweighted and weighted agreement factors of $R = \Sigma ||F_o| - |F_c|| / \Sigma |F_o|$ ($I > 2.00\sigma(I)$) and $wR = [\Sigma w(F_o^2 - F_c^2)^2 / \Sigma w(F_o^2)^2]^{1/2}$ were used. All calculations were performed by using the CrystalStructure[23] crystallographic software package except for refinement, which was performed by using SHELXL-97.[24]

Crystal data for TMβCD·TPyP: $C_{166}H_{250}N_8O_{70}$ (TPyP·2TMβCD); M_r 3477.77; crystal size $0.9 \times 0.3 \times 0.1$ mm; triclinic; $a = 16.864(4)$, $b = 17.532(4)$, $c = 17.712(4)$ Å; $\alpha = 98.9688(10)$, $\beta = 103.336(3)$, $\gamma = 112.917(2)°$; $V = 4514(2)$ Å^3; $T = 123(3)$ K; space group $P1$; $Z = 1$; $\rho_{calcd} = 1.279$ g cm^{-3}; $F_{000} = 1870.00$; $\lambda = 0.71070$ Å; $\mu(Mo_{K\alpha}) = 1.002$ cm^{-1}; $2\theta_{max} = 55.0°$; reflections collected: 36129, independent reflections: 19721 ($R_{int} = 0.0198$); final R indices ($I > 2.00\sigma(I)$) $R_1 = 0.0552$ and $wR_2 = 0.1383$; R indices (all data) $R_1 = 0.0677$ and $wR_2 = 0.1567$ with GOF = 1.059; largest diff. peaks and holes: 1.02 and −0.32 e Å^{-3}.

Crystal data for TMβCD·TCPP: $C_{174}H_{254}N_4O_{84}$ (TCPP·2TMβCD); M_r 3745.90; crystal size $0.160 \times 0.120 \times 0.060$ mm; monoclinic; $a = 16.983(2)$, $b = 28.298(3)$, $c = 20.715(2)$ Å; $\beta = 104.018(2)°$; $V = 9659(2)$ Å^3; $T = 193(1)$ K; space group $P2_1$; $Z = 2$; $\rho_{calcd} = 1.288$ g cm^{-3}; $F_{000} = 3996.00$; $\lambda = 0.71075$ Å; $\mu(Mo_{K\alpha}) = 1.027$ cm^{-1}; $2\theta_{max} = 54.9°$; reflections collected: 66789, independent reflections: 17319 ($R_{int} = 0.0350$); final R indices ($I > 2.00\sigma(I)$) $R_1 = 0.0666$ and $wR_2 = 0.1850$; R indices (all data) $R_1 = 0.0710$ and $wR_2 = 0.1908$ with GOF = 1.034; largest diff. peaks and holes: 0.72 and −0.50 e Å^{-3}.

Crystal data for TMβCD·TPP: $C_{170}H_{254}N_4O_{70}$ (TPP·2TMβCD); M_r 3473.86; crystal size $0.150 \times 0.120 \times 0.050$ mm; triclinic; $a = 16.8100$, $b = 17.9010$, $c = 17.7910$ Å; $\alpha = 98.0900$, $\beta = 102.3700$, $\gamma = 114.4900°$; $V = 4597.4571$ Å^3; $T = 113(1)$ K; space group $P1$; $Z = 1$; $\rho_{calcd} = 1.255$ g cm^{-3}; $F_{000} = 1862.00$; $\lambda = 0.71075$ Å; $\mu(Mo_{K\alpha}) = 0.970$ cm^{-1}; $2\theta_{max} = 58.2°$; reflections collected: 84580, independent reflections: 21063 ($R_{int} = 0.043$); final R indices ($I > 2.00\sigma(I)$) $R_1 = 0.0506$ and $wR_2 = 0.1053$; R indices (all data) $R = 0.0651$ and $wR_2 = 0.1152$ with GOF = 0.963; largest diff. peaks and holes: 0.87 and −0.33 e Å^{-3}.

Crystal data for TMβCD·Ni-TPP: $C_{170}H_{252}N_4NiO_{70}$ (Ni-TPP·2TMβCD); M_r 3530.55; crystal size $0.200 \times 0.200 \times 0.200$ mm; triclinic; $a = 16.782(3)$, $b = 17.880(3)$, $c = 17.794(3)$ Å; $\alpha = 98.078(2)$, $\beta = 102.593(2)$, $\gamma = 114.384(2)°$; $V = 4583.5(12)$ Å^3; $T = 93(1)$ K; space group $P1$; $Z = 1$; $\rho_{calcd} = 1.279$ g cm^{-3}; $F_{000} = 1888.00$; $\lambda = 0.71075$ Å; $\mu(Mo_{K\alpha}) = 1.970$ cm^{-1}; $2\theta_{max} = 62.0°$; reflections collected: 82886, independent reflections: 35088 ($R_{int} = 0.0309$); final R indices ($I > 2.00\sigma(I)$) $R_1 = 0.0426$ and $wR_2 = 0.1128$;

R indices (all data) $R = 0.0466$ and $wR_2 = 0.1171$ with GOF = 1.034; largest diff. peaks and holes: 1.11 and −0.48 e Å^{-3}.

CCDC-802112 (TMβCD·TPyP), CCDC-832805 (TMβCD·TCPP), CCDC-832806 (TMβCD·TPP), and CCDC-832807 (TMβCD·Ni-TPP) contain the supplementary crystallographic data for this paper. These data can be obtained free of charge from The Cambridge Crystallographic Data Centre via www.ccdc.cam.ac.uk/data_request/cif.

[1] Y. Tsuchiya, A. Ikeda, T. Konishi, J. Kikuchi, *J. Mater. Chem.* **2004**, *14*, 1128–1131.

[2] a) A. Huijser, T. J. Savenije, J. E. Kroeze, L. D. A. Siebbeles, *J. Phys. Chem. B* **2005**, *109*, 20166–20173; b) S. Eu, S. Hayashi, T. Umeyama, A. Oguro, M. Kawasaki, N. Kadota, Y. Matano, H. Imahori, *J. Phys. Chem. C* **2007**, *111*, 3528–3537.

[3] a) J. K. Klosterman, M. Iwamura, T. Tahara, M. Fujita, *J. Am. Chem. Soc.* **2009**, *131*, 9478–9479; b) Y. Inokuma, M. Kawano, M. Fujita, *Nat. Chem.* **2011**, *3*, 349–358.

[4] a) S. D. Karlen, M. A. García-Garibay, *Top. Curr. Chem.* **2005**, *262*, 179–227; b) B. Rodriguez-Molina, M. E. Ochoa, N. Farfán, R. Santillán, M. A. García-Garibay, *J. Org. Chem.* **2009**, *74*, 8554–8565.

[5] a) T. Hatano, A. Ikeda, T. Akiyama, S. Yamada, M. Sano, Y. Kanekiyo, S. Shinkai, *J. Chem. Soc. Perkin Trans. 2* **2000**, 909–912; b) A. Ikeda, T. Hatano, S. Shinkai, T. Akiyama, S. Yamada, *J. Am. Chem. Soc.* **2001**, *123*, 4855–4856.

[6] a) N. Kamiya, J.-R. Shen, *Proc. Natl. Acad. Sci. USA* **2003**, *100*, 98–103; b) Y. Umena, K. Kawakami, J.-R. Shen, N. Kamiya, *Nature* **2011**, *473*, 55–60.

[7] a) T. Kondo, T. Ito, S. Nomura, K. Uosaki, *Thin Solid Films* **1996**, *284/285*, 652–655; b) K. Uosaki, T. Kondo, X.-Q. Zhang, M. Yanagida, *J. Am. Chem. Soc.* **1997**, *119*, 8367–8368; c) H. Imahori, H. Norieda, S. Ozawa, K. Ushida, H. Yamada, T. Azuma, K. Tamaki, Y. Sakata, *Langumuir* **1998**, *14*, 5335–5338; d) A. Nomoto, Y. Kobuke, *Chem. Commun.* **2002**, 1104–1105.

[8] a) H. Inoue, S. Funyu, Y. Shimada, S. Takagi, *Pure Appl. Chem.* **2005**, *77*, 1019–1033; b) A. Satake, Y. Kobuke, *Org. Biomol. Chem.* **2007**, *5*, 1679–1691.

[9] K. Harata in *Cyclodextrins and Their Complexes* (Ed.: H. Dodziuk), Wiley-VCH, Weinheim, **2006**, pp. 147–198.

[10] a) H. Zhon, J. T. Groves, *J. Porphyrins Phthalocyanines* **2004**, *8*, 125–140; b) K. Kano, *Colloid Polym. Sci.* **2008**, *286*, 79–84; c) K. Kano, Y. Itoh, H. Kitagishi, T. Hayashi, S. Hirota, *J. Am. Chem. Soc.* **2008**, *130*, 8006–8015.

[11] A. Ikeda, T. Hatano, T. Konishi, J. Kikuchi, S. Shinkai, *Tetrahedron* **2003**, *59*, 3537–3540.

[12] a) S. Mosseri, J. C. Mialocq, B. Perly, *J. Phys. Chem.* **1991**, *95*, 2196–2203; b) T. Jiang, M. Li, D. S. Lawrence, *J. Org. Chem.* **1995**, *60*, 7293–7297; c) F. Venema, A. E. Rowman, R. J. M. Nolte, *J. Am. Chem. Soc.* **1996**, *118*, 257–258; d) T. Carofiglio, R. Fornasier, V. Lucchini, C. Rosso, U. Tonellato, *Tetrahedron Lett.* **1996**, *37*, 8019–8022; e) S. Hamai, T. Koshiyama, *J. Photochem. Photobiol. A* **1999**, *127*, 135–141; f) K. Kano, R. Nishiyabu, T. Asada, Y. Kuroda, *J. Am. Chem. Soc.* **2002**, *124*, 9937–9944.

[13] K. Kano, R. Nishiyabu, R. Doi, *J. Org. Chem.* **2005**, *70*, 3667–3673.

[14] J. S. Manka, D. S. Laurence, *J. Am. Chem. Soc.* **1990**, *112*, 2440–2442.

[15] a) K. Kano, N. Tanaka, H. Minamizono, Y. Kawakita, *Chem. Lett.* **1996**, 925–926; b) J. Mosinger, L. Slavětínská, K. Lang, P. Coufal, P. Kubát, *Org. Biomol. Chem.* **2009**, *7*, 3797–3804.

[16] Y. Tsuchiya, A. Yamano, T. Shiraki, K. Sada, S. Shinkai, *Chem. Lett.* **2011**, *40*, 99–101.

[17] Y. Takashima, Y. Oizumi, K. Sakamoto, M. Miyauchi, S. Kamitori, A. Harada, *Macromolecules* **2004**, *37*, 3962–3964.

[18] K. Komatsu, K. Fujiwara, Y. Murata, T. Braun, *J. Chem. Soc. Perkin Trans. 1* **1999**, 2963–2966.

[19] W. Jentzen, E. Unger, X.-Z. Song, S.-L. Jia, I. Turowska-Tyrk, R. Schweitzer-Stenner, W. Dreybrodt, W. R. Scheidt, J. A. Shelnutt, *J. Phys. Chem. A* **1997**, *101*, 5789–5798.

[20] K. Kano, H. Hasegawa, *J. Am. Chem. Soc.* **2001**, *123*, 10616–10627.

[21] P. Cosma, L. Catucci, P. Fini, P. L. Dentuto, A. Agostiano, N. Angelini, L. M. Scolaro, *Photochem. Photobiol.* **2006**, *82*, 563–569.

[22] a) S. Takagi, T. Shimada, M. Eguchi, T. Yui, H. Yoshida, D. A. Tryk, H. Inoue, *Langumuir* **2002**, *18*, 2265–2272; b) S. Takagi, M. Eguchi, D. A. Tryk, H. Inoue, *J. Photochem. Photobiol. C* **2006**, *7*, 104–126.

[23] CrystalStructure 4.0: Crystal Structure Analysis Package, Rigaku Corporation **2000–2010**.

[24] SHELX97: G. M. Sheldrick, *Acta Crystallogr. Sect. A* **2008**, *64*, 112–122.